OPEN

PRS GLOBAL OPEN

ORIGINAL ARTICLE
Peripheral Nerve

Biomechanical Evaluation of an Atraumatic Polymer-assisted Peripheral Nerve Repair System Compared with Conventional Neurorrhaphy Techniques

Alexie I. Wlodarczyk, MS, MEng*
Estelle C. Collin, MS, PhD*
Maria J.N. Pereira, PhD*
Randy Bindra, MBBS, FRACS, FRCS, MSOrth, MChOrth, FAOrthA†
Dominic M. Power, MA, MB, BChir (Cantab), FRCS (Trauma and Orth)‡

Background: Microsuturing, the gold standard for peripheral nerve repair, can create tension and damage at the repair site, potentially impacting regeneration and causing neuroma formation. A sutureless and atraumatic polymer-assisted system was developed to address this challenge and support peripheral nerve repair. The system is based on a biocompatible and biodegradable biosynthetic polymer and consists of a coaptation chamber and a light-activated polymer for securing to the nerve. In this study, we compare the system's biomechanical performance and mechanism of action to microsutures and fibrin repairs.

Methods: The system's fixation force was compared with microsutures and fibrin glue, and evaluated across various nerve diameters through tensile testing. Tension and tissue morphology at the repair site were assessed using finite element modeling and scanning electron microscopy.

Results: The fixation force of the polymer-assisted repair was equivalent to microsutures and superior to fibrin glue. This force increased linearly with nerve diameter, highlighting the correlation between polymer surface contact area and performance. Finite element modeling analysis showed stress concentration at the repair site for microsuture repairs, whereas the polymer-assisted repair dissipated stress along the nerve, away from the repair site. Morphological analysis revealed nerve alignment with no tissue trauma for the polymer-assisted repair, unlike microsutures.

Conclusions: The mechanical performance of the polymer-assisted coaptation system is suitable for peripheral nerve repair. The achieved fixation forces are equivalent to those of microsutures and superior to fibrin glue, minimizing stress concentration at the repair site and avoiding trauma to the severed nerve ends.
(Plast Reconstr Surg Glob Open 2024; 12:e6151; doi: 10.1097/GOX.0000000000006151; Published online 12 September 2024.)

INTRODUCTION

Annually, more than 700,000 individuals in the United States undergo surgery to address peripheral nerve injuries of various causes.[1,2] When left untreated, these injuries can lead to chronic pain, functional impairment, and a decline in the affected patients' quality of life.[3] Despite recent advances in treatment algorithms, managing peripheral nerve injuries still poses notable complexities. In particular, microsuture neurorrhaphy, currently the standard of care, has been associated with inconsistent results.[4,5] Advances in repair methodologies and new technologies are required to enhance patient outcomes.

Microsuture end-to-end neurorrhaphy is currently the standard of care for repair of a transected peripheral nerve. Microsutures provide the necessary tensile strength for nerve coaptation.[6,7] Nevertheless, microsuturing is associated with microtrauma, eliciting an intrafascicular inflammatory and fibrotic response, inducing tension and ischemia at the coaptation site, and leading to suboptimal fascicular alignment.[8,9] Microsuturing has a steep learning curve and needs extensive specialized surgical training.

*From *TISSIUM, Paris, France; †Griffith University School of Medicine and Dentistry, Gold Coast, Australia; and ‡Peripheral Nerve Surgery Department, Queen Elizabeth Hospital Birmingham, Birmingham, United Kingdom.*

Received for publication March 13, 2024; accepted July 24, 2024.

DOI: 10.1097/GOX.0000000000006151

Disclosure statements are at the end of this article, following the correspondence information.

The final quality of the repair, particularly in relation to fascicular alignment, has been demonstrated to be highly dependent on surgical expertise.[5,10] These different limitations of conventional repairs have been associated with impaired nerve regeneration and poor functional outcomes.

To overcome the inherent limitations of microsurgical neurorrhaphy, alternative technologies and techniques have been described. The combination of collagen conduits with microsutures (connector-assisted repair)[11,12] or the use of collagen conduits with embedded nitinol microhooks (Nerve Tape)[13,14] have been described to reduce tension and improve fascicular alignment. However, both techniques remain traumatic with foreign material piercing the nerve tissue, which can induce a similar inflammation and fibrosis response to that of microsutures.[13,15] In addition, connector-assisted repairs still require microsurgical techniques and, therefore, extensive training.[9] As an alternative, the use of glues or adhesive-based solutions has also been described, but safety and performance characteristics for these solutions have limited their adoption. In particular, fibrin glue has gained popularity for simplifying the surgical technique and providing atraumatic coaptation. However, it exhibits limited tensile strength and fast resorption, rendering it insufficient for standalone use in high-tension repairs.[6,16–20] Other adhesives described in the literature, such as cyanoacrylate, provide higher tensile strength but have been associated with local nerve toxicity, which negatively impacts nerve regeneration.[21–23]

We developed a polymer-assisted coaptation system designed to serve as a protective interface between the nerve and the surrounding tissues and to enable axonal growth across the repair site. It consists of two core components: (1) a 3D-printed coaptation chamber (Fig. 1A) and (2) a light-activated polymer (Fig. 1B). This polymer is applied in its prepolymer state, a thick gel, at the nerve/3D-printed coaptation chamber interface. Once in place, it polymerizes on demand within seconds by exposure to blue light, yielding a soft and flexible film that binds to tissues through mechanical interlocking.[24] Both components (3D-printed coaptation chamber and light-activated polymer) are derived from a photoactivated polymer based on a poly(glycerol sebacate) acrylate (PGSA) backbone.[25] This biocompatible and biodegradable polymer is derived from two naturally occurring compounds (glycerol and sebacic acid) in the human body. This polymer family, developed by TISSIUM, has been evaluated clinically as a vascular sealant.[26]

Takeaways

Question: Could a polymer-assisted nerve repair system provide sufficient fixation strength while allowing atraumatic and tensionless nerve repair?

Findings: The polymer-assisted nerve repairs group showed fixation strength equivalent to that of microsutures. This technology also preserved tissue architecture and offset tension from the neurorraphy site.

Meaning: The polymer-assisted nerve repair system is a promising alternative to microsutures and has the potential to improve outcomes of peripheral nerve repair.

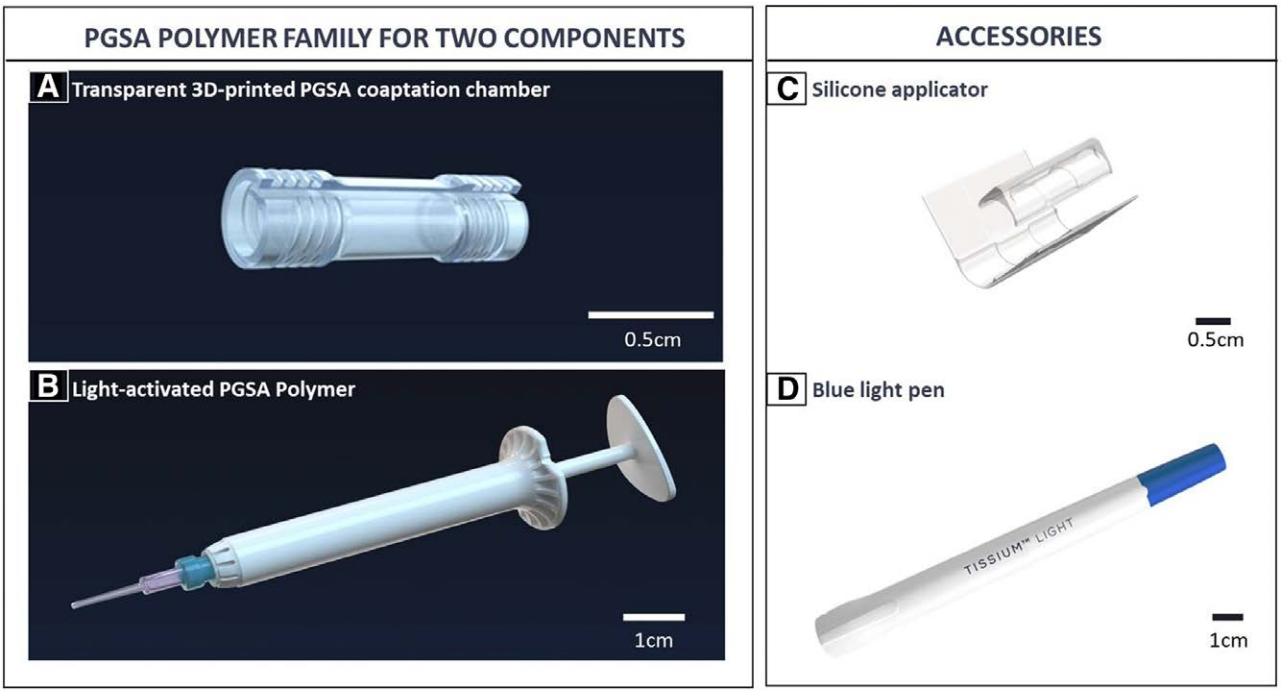

Fig. 1. Components of the polymer-assisted coaptation device and its accessories. The polymer-assisted coaptation device is a system composed of a 3D-printed chamber (A) and a light-activated polymer (B). A silicone applicator (C) and a blue light pen (D) enable the consistent application of the light-activated polymer and the polymerization in situ, respectively. Figure produced by TISSIUM.

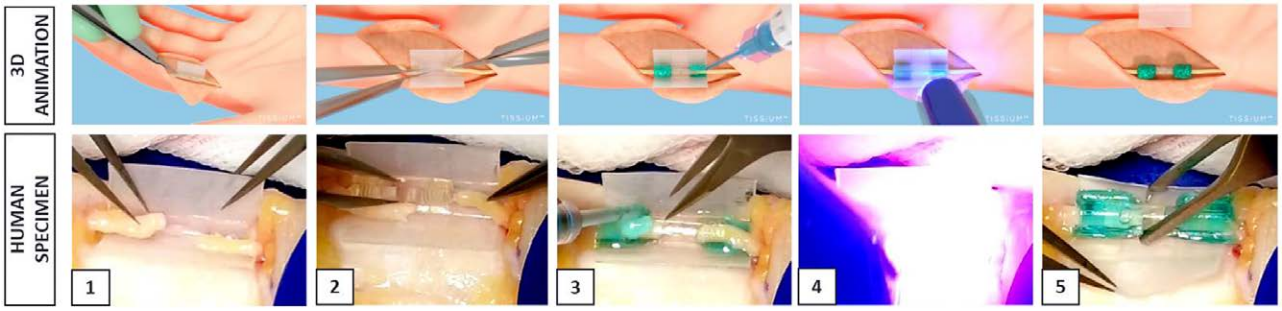

Fig. 2. The atraumatic repair of peripheral nerves with the polymer-assisted coaptation system is performed in five steps: (1) Placement of the silicone applicator as background; (2) insertion of the nerve ends and fascicle alignment within the 3D-printed coaptation chamber; (3) Application of the light-activated polymer; (4) on-demand polymerization of the light-activated polymer with the blue light pen; and (5) removal of the silicone applicator. Figure produced by TISSIUM.

The aim of this study is to characterize the biomechanical performances of the proposed polymer-assisted nerve coaptation system and compare it with microsuture neurorrhaphy and fibrin glue, as well as elucidate its mechanism of action via mechanical testing, numerical modeling, and image analysis.

MATERIALS AND METHODS

Biomechanical characterizations (mechanical testing and numerical modeling) were conducted using extracted nerves from different anatomical parts of rabbits, chickens, calves, and lambs to (1) evaluate performance of the polymer-assisted device against both microsutures, and fibrin glue repairs, (2) characterize the mechanical performance of the polymer-assisted device along a variable diameter range, and (3) numerically model the stress at the repair site. The interaction of the polymer-assisted device with the nerve tissue was evaluated using rat nerve extracted after acute in vivo implantation.

Polymer-assisted Coaptation System

The polymer-assisted coaptation system presented in this study, Coaptium Connect (TISSIUM, Paris), is composed of two different components: a three dimensional (3D)-printed coaptation chamber and a light-activated polymer. The 3D-printed coaptation chamber aims to guide the connection of severed nerve ends, alleviate tension at the coaptation site, and protect the repair to favor nerve regeneration.[9] It is designed as a translucent tubular wrap to facilitate the insertion of nerve ends. The light-activated polymer, prefilled in a single-use syringe, is used to attach the 3D-printed coaptation chamber to the proximal and distal segments of the injured nerve. It is applied using customized surgical instruments. Those surgical instruments include a syringe tip to precisely apply the light-activated polymer at the interface nerve/coaptation chamber, and a silicone applicator used to mold the light-activated polymer consistently around the nerve and the coaptation chamber. Briefly, using the textured grips as a visual indicator, at least 2.5 mm of the nerve ends are inserted into the coaptation chamber on each side. Once in place, the light-activated polymer is applied circumferentially at both nerve/coaptation chamber interfaces and polymerized in situ using a blue light pen (405 nm light emitting diode). All surfaces of the light-activated polymer must be exposed to one cycle of illumination (30 seconds) within a 2-cm working distance. The steps to deploy the system are summarized in Figure 2.

Biomechanical Tensile Testing

Sample Preparation to Evaluate the Repair Strength of the Polymer-assisted Repair System, Microsutures, and Fibrin

Uniaxial tensile testing was conducted to compare the performance of the polymer-assisted coaptation (n = 20) with microsutures (n = 10), and with fibrin glue (n = 10) using rabbit sciatic nerves (diameter of ~1.5 mm) purchased from a local butcher (see section "Uniaxial Tensile Testing" for uniaxial tensile test methodology). This testing model was chosen due to its resemblance in terms of diameter to that of human digital nerves and according to the 3Rs principles.[27,28] After extraction, the nerves were repaired with the selected method. The polymer-assisted repairs were carried out without microscope following the procedure described in section 1.1 and illustrated in Figure 2. Microsuture-assisted repairs were conducted by a peripheral nerve–trained surgeon, under microscope magnification (NexiusZoom EU 1760019, Euromex Microscopen B.V., Arnhem, The Netherlands). The neurorrhaphy was carried out using two epineurial stitches with 9-0 nylon microsutures (ETHILON 2809G BV130-5, Ethicon Inc., Raritan, N.J.). Fibrin glue-assisted repairs (Tisseel Fibrin Sealant, Baxter, Deerfield, Ill.) were performed in accordance with its instructions for use. In a temperature-controlled environment, the two nerve ends were aligned and, using a silicone application mold (length 2.5mm, thickness ~1 mm), the fibrin was applied to cover 2.5 mm in length on each nerve end all around the coaptation. The fibrin-assisted repairs were incubated at 37°C for at least 2 minutes before testing to induce coagulation of the fibrin components.

Sample Preparation to Evaluate the Impact of Light-activated Polymer Surface Contact Area on Mechanical Performance of the Polymer-assisted Repair System

Uniaxial tensile testing was used to assess the performance of the polymer-assisted repairs across variable surface contact areas with the nerve tissue (see section "Uniaxial

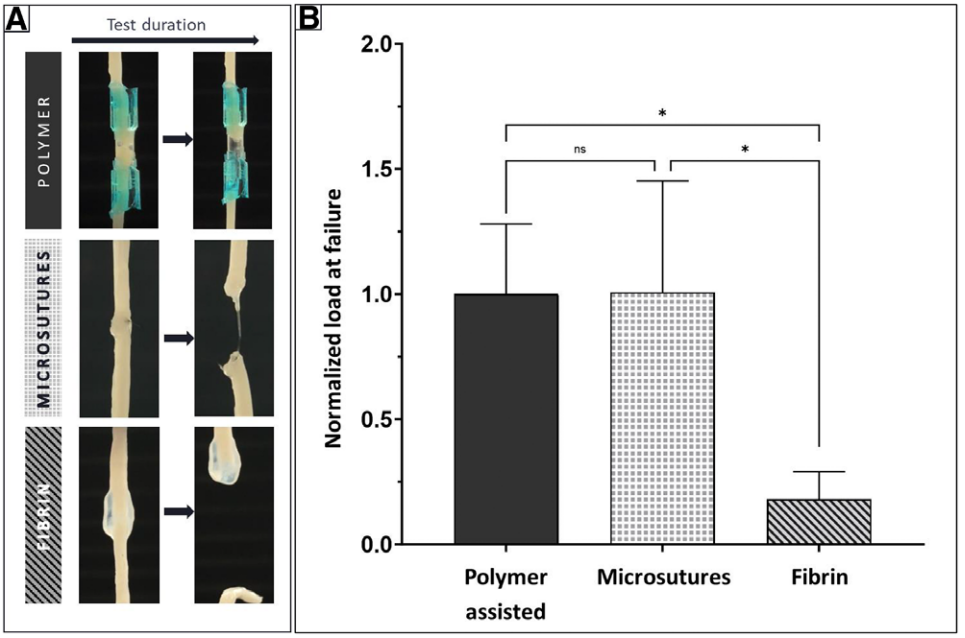

Fig. 3. Comparative analysis of repair strength. Repair strength of the polymer-assisted coaptation system is equivalent to microsutures, and superior to fibrin. (A) Representative images of nerve repairs undergoing uniaxial tensile test for polymer-assisted repairs (top), microsuture repairs (2 × 9-0) (middle), and fibrin-assisted repairs (bottom). (B) The load at failure following uniaxial tensile test is equivalent for the polymer-assisted and microsutures repairs. Data are shown as mean ± SD, statistical significance with $P < 0.05$. Figure produced by TISSIUM.

Tensile Testing" for uniaxial tensile test methodology). For this, nerves with diameters ranging from 1.5 to 6 mm were used as models. The nerves were isolated and harvested from different anatomical parts of chickens, calves, and lambs (n is five or more per diameter). The polymer-assisted repairs were conducted according to the previously described procedure (Fig. 2), using 3D-printed coaptation chambers sized according to the nerve diameter.

Uniaxial Tensile Testing

For both tests, each repaired specimen was kept moist and immediately mechanically tested. Nerve ends were clamped between pneumatic grips (Low-force grips 2712-051, Instron, Norwood, Mass.) loaded on 10N load cell (Series S-beam Static Load Cell 2519-10N, Instron, Norwood, Mass.) attached to a vertical mechanical testing machine (3340 Series Single Column, Instron, Norwood, Mass.). A uniaxial tensile test was performed at the rate of 10 mm per min, with repair failure as the test stop criterion (Fig. 3A). The maximum load reached at the point of repair failure (load at failure) was recorded, along with the failure mode.

Stress Concentration Modeling through Finite Element Analysis

A scenario of uniaxial tensile load case was replicated through finite elements modeling [HyperWorks Altair software (2023)] on (1) polymer-assisted and (2) microsuture-assisted nerve repair. The nerve was modeled as a cylinder separated in two parts: an inner nerve trunk and an outer membrane (epineurium). For the microsuture-assisted repair, two epineurial suture holes were placed 0.25 mm away from the neurorrhaphy site. All materials were considered linear elastic. The nerve mechanical properties (E, ν) were estimated using Koppaka et al as reference.[29] The nerve trunk was considered as a homogenous structure with the same mechanical properties as the perineurium. The resulting forces at the symmetry plane, the displacement of the nerve extremity, and the Von Mises stress distribution were measured. Stress distribution along the coaptation was represented with different colored indicators from high area of stress (red) to low area of stress (blue).

Interaction with Biological Tissues through Scanning Electron Microscopy

Experiments were conducted in accordance with the French National Ethical guidelines under the agreement #31534. Six adult Wistar Han female rats (Janvier Labs, Le Genest-Saint-Isle, France), reused following the 3Rs principles,[27] weighing approximately 300 g, were administrated buprenorphine (0.05 mg/kg) and meloxicam (2 mg/kg) previously anesthetized under isoflurane gas. A 2-cm longitudinal incision was performed in the skin below the femur, and the sciatic nerve was exposed. The end of the *linea aspera* extending from the tertiary trochanter of the femur was used as a landmark to transversely section the sciatic nerve. Polymer-assisted nerve repairs followed the procedure previously described (Fig. 2). Microsuture repairs consisted of two epineurial stitches with 9-0 nylon

microsutures (ETHILON 2809G BV130-5, Ethicon Inc., Raritan, N.J.). The rats were euthanized after surgery by CO_2 inhalation. All repaired sciatic nerves were harvested immediately after euthanasia, fixed in 4% glutaraldehyde, and stored at 4°C for at least 24 hours. After fixation, samples were prepared for microscopic observations and imaged using a scanning electron microscope (JCM-6000Plus microscope and software v.1.4.0, JEOL Ltd., Tokyo, Japan).

Statistical Analysis

Graphs and statistical analysis were performed on GraphPad Prism v.9 (GraphPad Software Inc., La Jolla, Calif.). For both comparisons, normality was assessed using a Kolmogorov-Smirnov normality test. Normality was observed for both experimental sets ($P > 0.1$). Because variances were nonhomogeneous, differences between the groups were analyzed by Welch's analysis of variance (ANOVA) test followed by Dunnett T3 post hoc test for multiple comparisons. The following thresholds for statistical significance were considered at $P < 0.05$. Data are reported as mean ± SD.

RESULTS

Comparison of Repair Strength of the Polymer-assisted Repair System, Microsutures, and Fibrin Glue

The biomechanical performance of the polymer-assisted system was compared with both microsuture neurorrhaphy, and fibrin glue through uniaxial tensile testing. The average repair strength of microsutures was statistically equivalent to polymer-assisted repairs ($P > 0.05$). Both were significantly superior (approximately five-fold) to fibrin-assisted repairs ($P < 0.05$), as illustrated in Figure 3B. Microsuture-assisted repairs failed due to epineurium rupture (n = 9) or knot opening (n = 1), whereas polymer-assisted and fibrin-assisted repairs failed due to the loss of contact between the epineurium and polymer, without disruption to the tissue.

Impact of Surface Contact Area on the Mechanical Performance of the Polymer-assisted Repair System

The repair strength of the polymer-assisted system relies on the surface contact area of light-activated polymer in contact with the tissue. Therefore, it was hypothesized that the larger the surface contact area with the tissue, the higher the repair strength would be. To validate this hypothesis, the load at failure was measured across various nerve diameters, which inherently have varying surface contact areas with the light-activated polymer. Load at failure was observed to increase linearly with nerve diameter, highlighting the correlation of the repair strength of the polymer-assisted system and the light-activated polymer surface contact area ($R^2 > 0.98$). For instance, for nerves of 6mm in diameter, the load at failure was four-fold higher than for nerves of 1.5 mm in diameter ($P < 0.05$, Fig. 4). This result highlights the positive impact of contact surface area between the light-activated polymer and nerve tissue on repair strength.

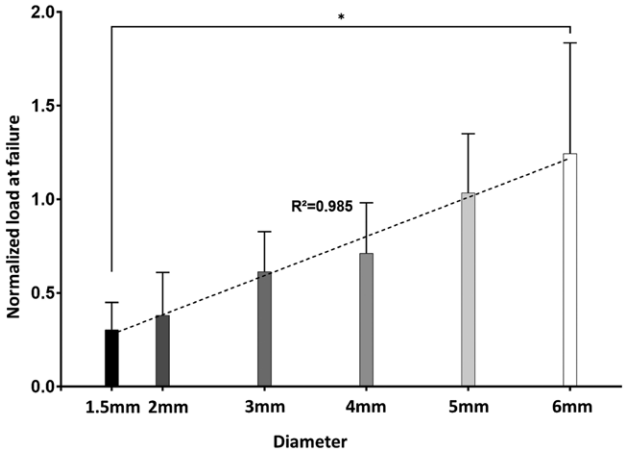

Fig. 4. Polymer-assisted repair strength linearly increases with its surface contact area. Data are shown as mean ± SD, statistical significance with *P* less than 0.05. Figure produced by TISSIUM.

Stress Concentration Modeling through Finite Element Analysis

Finite element modeling of a uniaxial tensile loading (0.1N) scenario on direct microsutures repair demonstrated a maximum stress localized on the puncture site of microsutures through the epineurium (red). The polymer-assisted solution displayed a 12-fold lower maximum stress, evenly distributed along the nerve diameter, away from the coaptation site (blue/yellow) (Fig. 5A.). In contrast to the microsuture neurorrhaphy, the polymer-assisted system showed a de-tensioning of the coaptation.

Interaction of the Different Repair Methods with Biological Tissues through Scanning Electron Microscopy

The interaction between the polymer-assisted repair system and the nerve tissue was assessed both macroscopically and via scanning electron microscopy (SEM) after acute implantation in a rat model. A lack of alignment of nerve ends was observed only for the microsuture-assisted repairs (Fig. 5A). SEM highlighted the preservation of the tissue structure for the polymer-assisted repairs, with the light-activated polymer layer mechanically interlocking with the epineurium. Conversely, microsuture repairs disrupt the integrity of the epineurium and potentially its sublayers (perineurium and endoneurium), as shown in Figure 5B.

DISCUSSION

The field of plastic and orthopedic surgery presents an increased interest in the development and application of innovative technologies for diagnostics and therapeutics.[30–34] Those technologies have the potential to improve patient outcomes and reduce healthcare costs. Specifically, in the field of hand and microsurgery, peripheral nerve surgeons have highlighted the need for alternative and more reliable peripheral nerve repair techniques to improve outcomes.[9,35] Indeed, microsutures, the current standard of care, have been associated with impaired peripheral nerve regeneration and neuroma formation

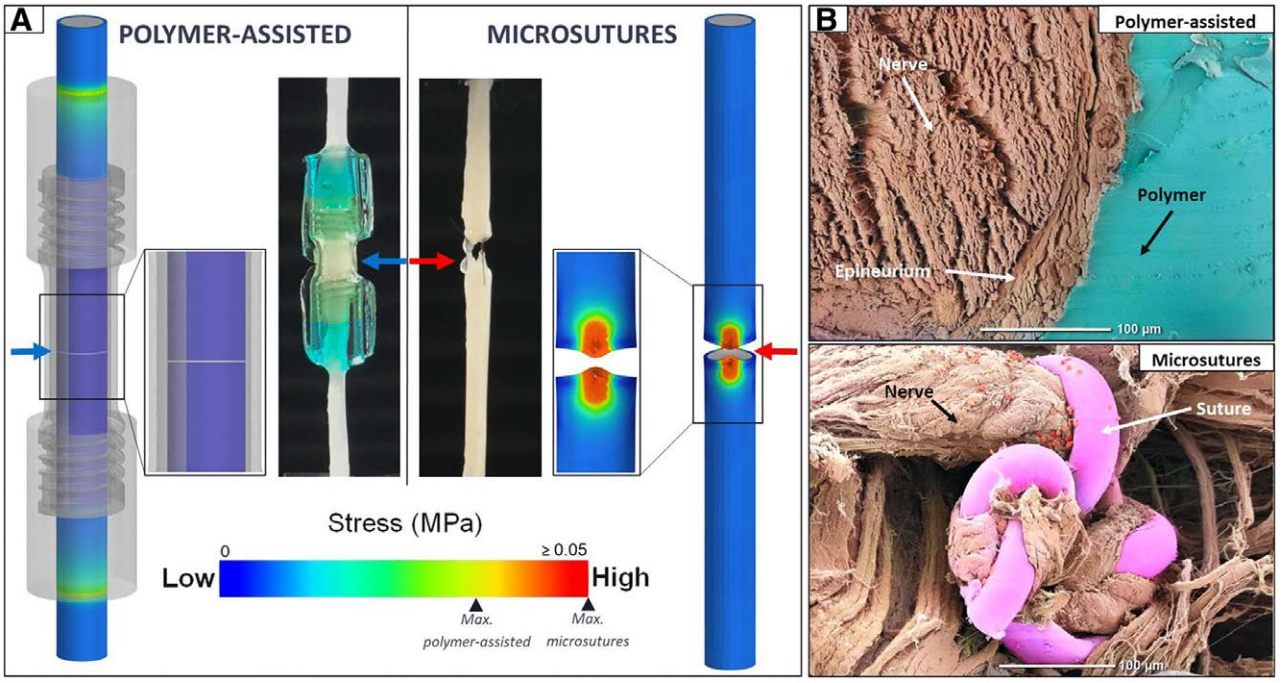

Fig. 5. Evaluation of stress distribution and tissue interaction with polymer-assisted and microsuture-assisted repairs. The polymer-assisted coaptation system enables atraumatic and tensionless peripheral nerve repair. (A) FEM of peripheral nerve exposed to tensile forces demonstrate that stress dissipation in the case of the polymer-assisted repair, while stress concentration is observed on coaptation site when using microsutures. Arrows indicate neurorrhaphy location. (B) Colorized SEM representative image of the polymer–tissue interface, demonstrating the atraumatic nature of the polymer-assisted repair. The light-activated polymer mechanically interlocks with the tissue surface and maintains the tissue anatomy, while microsutures penetrate and disrupt the tissue layers. Figure produced by TISSIUM.

by (1) inducing localized trauma to the nerve and reactive scarring due to foreign material at and within the anastomosis site, (2) concentrating tension around the repair site, and (3) impairing fascicular alignment while approximating nerve ends.[5,8–10,36,37] Microsutures are also technically challenging and require extensive microsurgical training that can impact consistency of outcomes. Therefore, alternatives to microsuture repairs have been explored in recent years.[6,8,13,14,38] An optimal peripheral nerve repair system should provide equivalent repair strength to microsutures in a tensionless and atraumatic manner for the nerve, enabling fascicular alignment and maintaining the nerve architecture.[8,13–15]

In this study, we report the development and characterization of an atraumatic sutureless polymer-assisted system to support peripheral nerve repair. The polymer-assisted system presented is composed of a 3D-printed coaptation chamber and a light-activated polymer. The 3D-printed coaptation chamber was designed to facilitate the insertion, alignment while reapproximating the severed nerve ends (Fig. 5). Its fixation to the nerve using the light-activated polymer minimizes tension at the repair site and additional trauma to the nerve (Fig. 1A.). Additionally, its transparency allows for the visualization of the nerve ends, aiding in the positioning of the nerve ends and the alignment of fascicles (Fig. 2). This contrasts with other peripheral nerve repair devices such as conduits or connectors which are opaque and do not allow the assessment of fascicular alignment during the surgical procedure.[10] The polymer-assisted system was designed to preserve nerve tissue architecture while creating a strong bond to the coaptation chamber and the nerve.

Although the optimal strength required for peripheral nerve repair remains uncertain, it is generally accepted that employing one to two microsutures with a range of gauges from 10-0 to 8-0 is sufficient for a robust repair of digital nerves, the most frequently injured nerves.[6,7,39,40] In this study, we selected a repair technique using two epineurial stitches of 9-0 nylon microsuture as a control, which is commonly used for digital nerve repairs that have a similar diameter to the nerves used here.[41,42] The proposed polymer-assisted system presents equivalent repair strength (load at failure) to that of the microsutures (Fig. 3). Furthermore, both the polymer-assisted system and microsutures exhibit a load at failure five-fold superior to fibrin glue. These findings align with previous reports in which fibrin glue, when used alone as an alternative to microsutures, presents lower biomechanical performance than microsutures[20] and highlight that the proposed polymer-assisted system provides adequate repair strength for clinical translation.

The mechanism of action of the polymer-assisted system involves fixation by mechanically interlocking with the tissue surface.[24,26] Consequently, the strength relies on the contact surface area between the light-activated polymer and the tissue.[43] The polymer-assisted system enhances the repair strength as the nerve diameter increases, which is expected as the surface contact area between the nerve tissue and

the light-activated polymer increases. This effect leads to a positive correlation between nerve diameter/surface contact area and load at failure (Fig. 4). This atraumatic fixation mechanism of the light-activated polymer allows the alignment and architecture of the nerve to remain intact as observed on the SEM micrographs, limiting the risk of trauma to the tissue that can be observed with microsutures (Fig. 5B). The technique of microsuture neurorrhaphy, due to its penetrative nature, has been associated with intrafascicular inflammatory and fibrotic responses as well as with a suboptimal fascicular alignment at the coaptation site.[8,9] Additional in vivo studies are necessary to confirm that the atraumatic nature of the polymer-assisted repair system reduces inflammation and fibrosis within the nerve tissue while supporting nerve regeneration.

Nerve repair technique is also known to influence tension at the repair site. Tension is known to result in local ischemia, reduction of Schwann cell proliferation, fibrosis, and scarring, similar to the effects of microsuture penetration that can impair functional outcomes.[36,44,45] In recent years, de-tensioning repair techniques have gained prominence as a means to enhance functional regeneration in preclinical and clinical settings.[9,10,46] Finite element modeling evidence suggests that the polymer-assisted system alleviates tension from the coaptation site when subjected to a load, whereas, as expected,[9] microsuture repairs result in stress concentration around the microsutures and, therefore, tension at the repair site (Fig 5. A).

This study is not without limitations. The biological tissues used in this study are animal nerves and not human cadaveric nerves, and are therefore less representative of the final application. Tests were also performed immediately after repair. In vivo studies will be required to determine the biological response over time.

CONCLUSIONS

Peripheral nerve repair with the polymer-assisted system demonstrates retention strength comparable to current standard-of-care microsutures while surpassing the performance of fibrin glue. An essential benefit of this system is its ability to effectively reduce stress concentration (tension) at the repair site while preserving the structural integrity to the severed nerve end. The atraumatic and de-tensioning features of the polymer-assisted system are believed to create a protective interface and optimized biomechanical environment for nerve regeneration. This technology is a promising alternative to microsuture-assisted peripheral nerve repair, and further studies will allow validating its functional outcomes.

Maria J.N. Pereira, PhD
TISSIUM
74 rue du Faubourg Saint Antoine
75012 Paris, France
mpereira@tissium.com

DISCLOSURES

Alexie I. Wlodarczyk and Estelle C. Collin are employees of TISSIUM and have received salaries and other compensation in connection with the employment. Maria Pereira is an employee and co-founder of TISSIUM and has received salaries and other compensation in connection with the employment. Randy Bindra is consultant for Acumed and TISSIUM, paid speaker for Acumed & Smith and Nephew, and receive royalties from Acumed. Dominic Power provides consulting services to the biomedical technology sector for advice on product design, usability testing, and clinical trial design. He has received consulting fees from TISSIUM.

TISSIUM is the sponsor of this study and has provided financial support for the conduct of the research and preparation of the article.

REFERENCES

1. Grand View Report. Peripheral Nerve Injuries Market Size & Share Report, 2030. Available at https://www.grandviewresearch.com/industry-analysis/peripheral-nerve-injuries-market-report. March 1, 2024. Accessed August 6, 2024.
2. Kouyoumdjian JA. Peripheral nerve injuries: a retrospective survey of 456 cases. *Muscle Nerve.* 2006;34:785–788.
3. Dahlin LB, Wiberg M. Nerve injuries of the upper extremity and hand. *EFORT Open Rev.* 2017;2:158–170.
4. Kim DH, Han K, Tiel RL, et al. Surgical outcomes of 654 ulnar nerve lesions. *J Neurosurg.* 2003;98:993–1004.
5. Isaacs J, Safa B, Evans PJ, et al. Technical assessment of connector-assisted nerve repair. *J Hand Surg.* 2016;41:760–766.
6. Isaacs JE, McDaniel CO, Owen JR, et al. Comparative analysis of biomechanical performance of available "nerve glues." *J Hand Surg.* 2008;33:893–899.
7. Giddins G, Wade P, Amis A. Primary nerve repair: Strength of repair with different gauges of nylon suture material. *J Hand Surg.* 1989;14:301–302.
8. Barton MJ, Morley JW, Stoodley MA, et al. Nerve repair: toward a sutureless approach. *Neurosurg Rev.* 2014;37:585–595.
9. Nassimizadeh M, Nassimizadeh AK, Power D. Managing the nerve gap: new tools in the peripheral nerve repair toolbox. *J Med Sci Res.* 2019;3:4.
10. Ducic I, Safa B, DeVinney E. Refinements of nerve repair with connector-assisted coaptation. *Microsurgery.* 2017;37:256–263.
11. Boeckstyns ME, Sørensen AI, Viñeta JF, et al. Collagen conduit versus microsurgical neurorrhaphy: 2-year follow-up of a prospective, blinded clinical and electrophysiological multicenter randomized, controlled trial. *J Hand Surg Am.* 2013;38:2405–2411.
12. Taras JS, Jacoby SM, Lincoski CJ. Reconstruction of digital nerves with collagen conduits. *J Hand Surg.* 2011;36:1441–1446.
13. Bendale G, Smith M, Daniel L, et al. In vivo efficacy of a novel, sutureless coaptation device for repairing peripheral nerve defects. *Tissue Eng Part A.* 2023;29:461–470.
14. Bendale GS, Sonntag M, Clements IP, et al. Biomechanical testing of a novel device for sutureless nerve repair. *Tissue Eng Part C Methods.* 2022;28:469–475.
15. Tse R, Ko JH. Nerve glue for upper extremity reconstruction. *Hand Clin.* 2012;28:529–540.
16. Koopman JE, Duraku LS, de Jong T, et al. A systematic review and meta-analysis on the use of fibrin glue in peripheral nerve repair: can we just glue it? *J Plast Reconstr Aesthet Surg.* 2022;75:1018–1033.
17. Sameem M, Wood TJ, Bain JR. A systematic review on the use of fibrin glue for peripheral nerve repair. *Plast Reconstr Surg.* 2011;127:2381–2390.
18. Bhandari PS. Use of fibrin glue in the repair of brachial plexus and peripheral nerve injuries. *Indian J Neurotrauma.* 2013;10:30–32.
19. Hweidi SA, Elsayed GY. Comparison between conventional microsurgical technique and fibrin glue in repair of peripheral nerve injuries. *Egypt J Plast Reconstr Surg.* 2012;36:233–238.

20. Temple CLF, Ross DC, Dunning CE, et al. Resistance to disruption and gapping of peripheral nerve repairs: an in vitro biomechanical assessment of techniques. *J Reconstr Microsurg.* 2004;20:645–650.
21. Wieken K, Angioi-Duprez K, Lim A, et al. Nerve anastomosis with glue: comparative histologic study of fibrin and cyanoacrylate glue. *J Reconstr Microsurg.* 2003;19:17–20.
22. Landegren T, Risling M, Persson JKE, et al. Cyanoacrylate in nerve repair: transient cytotoxic effect. *Int J Oral Maxillofac Surg.* 2010;39:705–712.
23. Chow N, Miears H, Cox C, et al. Fibrin glue and its alternatives in peripheral nerve repair. *Ann Plast Surg.* 2021;86:103–108.
24. Lang N, Pereira MJ, Lee Y, et al. A blood-resistant surgical glue for minimally invasive repair of vessels and heart defects. *Sci Transl Med.* 2014;6:p218ra6.
25. Pereira MJN, Ouyang B, Sundback CA, et al. A highly tunable biocompatible and multifunctional biodegradable elastomer. *Adv Mater.* 2013;25:1209–1215.
26. Pellenc Q, Touma J, Coscas R, et al. Preclinical and clinical evaluation of a novel synthetic bioresorbable, on-demand, light-activated sealant in vascular reconstruction. *J Cardiovasc Surg.* 2019;60:599–611.
27. Hubrecht RC, Carter E. The 3Rs and humane experimental technique: implementing change. *Animals.* 2019;9:754.
28. Merolli A, Li M, Voronin G, et al. A sciatic nerve gap-injury model in the rabbit. *J Mater Sci Mater Med.* 2022;33:14.
29. Koppaka S, Hess-Dunning A, Tyler DJ. Biomechanical characterization of isolated epineurial and perineurial membranes of rabbit sciatic nerve. *J Biomech.* 2022;136:111058.
30. Guarro G, Cozzani F, Rossini M, et al. The modified TIME-H scoring system, a versatile tool in wound management practice: a preliminary report. *Acta Biomed.* 2021;92:e2021226.
31. Glauser G, Winter E, Caplan IF, et al. The LACE+ index as a predictor of 30 day patient outcomes in a urologic surgery population: a coarsened exact match study. *Urology.* 2019;134:109–115.
32. Guarro G, Cozzani F, Rossini M, et al. Wounds morphologic assessment: application and reproducibility of a virtual measuring system, pilot study. *Acta Biomed.* 2021;92:e2021227.
33. Baccarani A, Pappalardo M, Ceccarelli PL, et al. Combined double-breasted full-thickness abdominal flap plication and acellular dermal matrix in prune-belly syndrome reconstruction. *Plast Reconstr Surg Glob Open.* 2024;12:e5744.
34. Shilo D, Capucha T, Krasovsky A, et al. Real-time reconstruction of comminuted mandibular fractures using 3D printing. *Plast Reconstr Surg Glob Open.* 2024;12:e5645.
35. Owusu A, Mayeda B, Isaacs J. Surgeon perspectives on alternative nerve repair techniques. *Hand (New York, N,Y.).* 2014;9:29–35.
36. Dvali L, Mackinnon S. The role of microsurgery in nerve repair and nerve grafting. *Hand Clin.* 2007;23:73–81.
37. Braga Silva J, Becker AS, Leal BLM, et al. Advances of direct peripheral nerve repair techniques: do we already have enough scientific evidence? *Indian J Orthop.* 2023;57:189–202.
38. Benfield C, Isaacs J, Mallu S, et al. Comparison of nylon suture versus 2 fibrin glue products for delayed nerve coaptation in an animal model. *J Hand Surg.* 2021;46:119–125.
39. Sunderland IR, Brenner MJ, Singham J, et al. Effect of tension on nerve regeneration in rat sciatic nerve transection model. *Ann Plast Surg.* 2004;53:382–387.
40. Mermans JF, Franssen BBGM, Serroyen J, et al. Digital nerve injuries: a review of predictors of sensory recovery after microsurgical digital nerve repair. *Hand.* 2012;7:233–241.
41. Goldberg SH, Jobin CM, Hayes AG, et al. Biomechanics and histology of intact and repaired digital nerves: an in vitro study. *J Hand Surg.* 2007;32:474–482.
42. Beris A, Gkiatas I, Gelalis I, et al. Current concepts in peripheral nerve surgery. *Eur J Orthop Surg Traumatol.* 2019;29:263–269.
43. Pujari-Palmer M, Giró R, Procter P, et al. Factors that determine the adhesive strength in a bioinspired bone tissue adhesive. *ChemEngineering.* 2020;4:19.
44. Yi C, Dahlin LB. Impaired nerve regeneration and Schwann cell activation after repair with tension. *Neuroreport.* 2010;21:958–962.
45. Israel JS, Dingle AM, Pisaniello JA, et al. Recovery and regrowth after nerve repair: a systematic analysis of four repair techniques. *J Surg Res.* 2020;251:311–320.
46. Schmidhammer R, Zandieh S, Hopf R, et al. Alleviated tension at the repair site enhances functional regeneration: the effect of full range of motion mobilization on the regeneration of peripheral nerves–histologic, electrophysiologic, and functional results in a rat model. *J Trauma.* 2004;56:571–584.